

Fourth European Rotorcraft and Powered-Lift Aircraft Forum

Paper No. 22

**ON METHODS FOR APPLICATION
OF HARMONIC CONTROL**

E.R. Wood and R.W. Powers
Hughes Helicopters
Culver City, California USA

and

C.E. Hammond
Structures Laboratory
U.S. Army Research & Technology Laboratories
(Aviation Research and Development Command)
NASA Langley Research Center,
Hampton, Virginia USA

September 13-15, 1978
Stresa – Italy

Associazione Italiana di Aeronautica ed Astronautica
Associazione Industrie Aerospaziali

ON METHODS FOR APPLICATION OF HARMONIC CONTROL

E. R. Wood and R. W. Powers
Hughes Helicopters
Culver City, California USA

and

C. E. Hammond
Structures Laboratory
U. S. Army Research & Technology Laboratories
(Aviation Research and Development Command)
NASA Langley Research Center,
Hampton, Virginia USA

Abstract

Over the past several years the NASA Langley Research Center and the Structures Laboratory, USARTL, has undertaken a comprehensive program to reevaluate higher harmonic blade pitch control for helicopter vibration reduction. Hughes Helicopters under contract¹ has been tasked with providing analyses and computer programs to sense and suppress vibratory excitation in either the open or closed loop mode. Data presented in the paper confirm the effectiveness of higher harmonic blade pitch control in substantially reducing rotor vibratory hub loads. The data are the result of recent tests on a 2.7-m (9-ft) diameter, four-bladed articulated rotor model that were conducted in the Langley Research Center's transonic dynamics wind tunnel. Several predictive analyses developed in support of the NASA program are shown capable of accurately predicting both amplitude and phase of the higher harmonic control input required to nullify a single 4/rev force or moment input. The paper also discusses the more general analysis, that of multiple blade feathering inputs to attenuate multiple vibratory forces and moments, and its application for design of a flightworthy higher harmonic control system.

Notation

Definition of notation is expanded within the text as the algorithms are developed. Given below is the definition of symbols that are fundamental to the paper:

F _x	Fore and aft vibratory hub force at nΩ frequency
F _y	Lateral vibratory hub force at nΩ frequency

¹ Work reported on in this paper is being performed under NASA Contract No. NAS1-14552, jointly funded by NASA and USARTL.

F _z	Vertical vibratory force at nΩ frequency
M _{xx}	Vibratory hub rolling moment at nΩ frequency
M _{yy}	Vibratory hub pitching moment at nΩ frequency
M _{zz}	Vibratory hub yawing moment at nΩ frequency
Z	Vertical displacement of the stationary swashplate at nΩ frequency
θ	Pitch angle (longitudinal) of the stationary swashplate at nΩ frequency
φ	Roll angle (lateral) of the stationary swashplate at nΩ frequency

Subscripts

C	Cosine component
S	Sine component
BL	Baseline (ambient vibratory case, no swashplate excitation)

1. Introduction

Vibration plays a major role in the design and development of the modern-day helicopter. Frequently the success or failure of a helicopter has been governed by whether or not it met vibration requirements. Low vibration levels are important both for crew and passenger comfort, as well as to reduce fatigue of airframe and dynamic components. In transmitting vibratory forces from the rotor to the airframe, the rotor system acts as a filter. This results in primary excitation to the airframe occurring at the blade passage frequency of n/rev where "n" is the number of blades.

For a four-bladed rotor, higher harmonic control (HHC) achieves reduction of airframe

4/rev vibration levels by superposition of perturbations of 3, 4, and 5/rev blade feathering on the basic 1/rev cyclic pitch required for helicopter trim. While the concept is not new, only recently has it been shown feasible. In particular, results of experimental efforts described in References 1, 2, 3, 4, and 5 have shown that successful suppression of vibration can be achieved by oscillating the blades at relatively small angles, generally less than 0.5 degree. These results are highly encouraging because they indicate that successful vibration reduction can be achieved with no significant penalties in blade flap bending, push-rod loads, or rotor performance.

Further, it would appear that technology has advanced to the point where higher harmonic control offers the next logical step for alleviating helicopter vibrations. Consider Figure 1, which shows the trend of helicopter cockpit vibration levels over the past twenty-five years. Observe that the helicopter industry has reached an asymptote in the level of vibration reduction that can be achieved by present methods. Desired² is a level of 0.02g, one-fifth that attainable with today's technology. The authors believe that such levels can be realized only by a major breakthrough in vibration reduction techniques. Higher harmonic control offers one method that promises such a breakthrough.

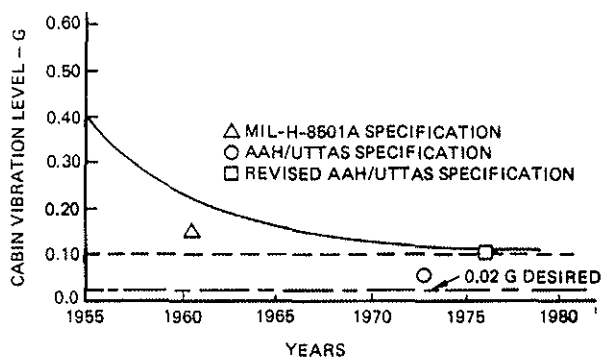


Figure 1. Trend of Helicopter Vibration Levels Since 1955

While early attempts at higher harmonic control had to rely on purely mechanical devices (Reference 6), there have been two advances in the past ten years that both eliminate the need for such devices and simultaneously offer great promise toward development of a practical, flightworthy higher harmonic control system.

These are: (1) the advent of the high-speed, lightweight microprocessor; and (2) development of Fast Fourier Transform methods for spectral analysis (References 7, 8 and 9). Both are essential to implement an active rotor vibration control system. The system described has the capability to:

- Sample vibratory hub loads.
- Convert these analog signals to digitized data (A to D converter).
- Separate amplitude and phase of n/rev components by Fast Fourier Transform methods (microprocessor).
- From several samplings use the appropriate algorithm to determine amplitude and phase of rotor higher harmonic feathering inputs to null vibratory hub loads (microprocessor).
- Convert resulting digitized input to an analog signal (D to A converter).
- Amplify and feed resulting higher harmonic signals into the helicopter's primary control system servos.

Over the past several years the NASA Langley Research Center and the Structures Laboratory, USARTL, has undertaken a comprehensive program to reevaluate higher harmonic blade pitch control for helicopter vibration reduction. Hughes Helicopters under contract to NASA and Army has been tasked with providing analyses and computer programs for supporting wind tunnel data reduction. As an extension of this effort, Hughes Helicopters is also working with NASA and Army on the implementation of analyses to sense and suppress vibratory excitation in either the open or closed loop mode.

The NASA/Army/Hughes effort is directed toward systematic development of a flightworthy active vibration control system. The purpose of initial phases of the project has been to explore the effectiveness of various solution techniques (algorithms) in determining the control inputs required for reducing hub-transmitted forces. This has been accomplished by tests using a 2.7-m (9-ft) diameter, four-bladed aeroelastically-scaled articulated rotor. Tests have been conducted in the NASA/Langley 5-m (16-ft) transonic dynamics wind tunnel (TDT) (see Figure 2). The TDT facility has the unique capability of using either Freon-12 or air as the fluid medium. The advantages of Freon-12 as a test medium for aeroelastic testing of scale model rotors has been discussed in Reference 17.

² Recommended by NASA Research and Technology Advisory Council Subpanel on Helicopter Technology, Washington, D. C., May 24, 1976.

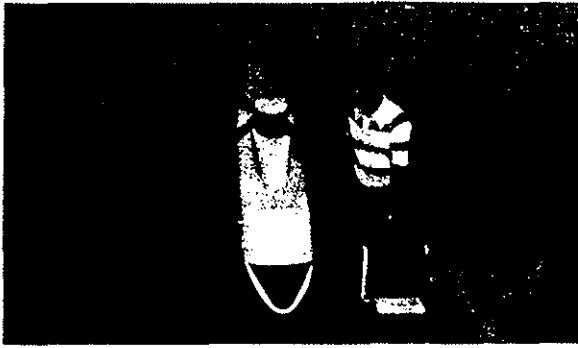


Figure 2. NASA/Army Aeroelastic Rotor Experimental System (ARES)

For data reduction and analysis, the model and its instrumentation are linked to a Xerox Sigma 5 data acquisition system, especially designed to support aeroelastic research.

An outline of the research now under way is presented in Figure 3. This paper is a status report of work to date. In addition the paper will address such topics as:

- Characteristics of alternative mathematical algorithms especially developed to generate required swashplate inputs from sampled vibratory force data so as to minimize airframe vibration.
- Reduction of coupled rotor hub forces and moments with multiple vibratory swashplate input.

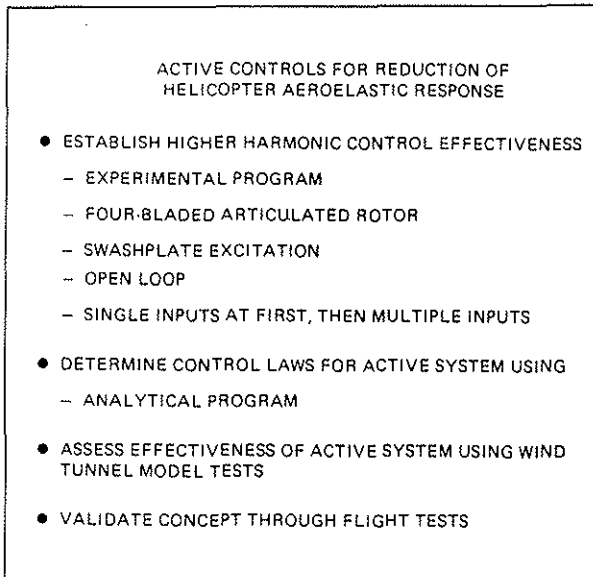


Figure 3. NASA/Army Active Higher Harmonic Control Program

- Design application of higher harmonic blade feathering as an active feedback control system in an OH-6A helicopter.

2. Background

For airframe vibrations that occur at integral multiples of rotor speed, the principal source is the rotor system. Here, harmonics of aerodynamic loads on the blade give rise to vibratory response of the blade. Since the blade is restrained at the root, blade responses result in root shears and moments, which feed from the rotor hub to the airframe as vibratory shears and moments.

As the forces go from the rotating to the fixed fuselage system, the rotor system in steady-state flight acts as a filter. For an n -bladed rotor system, the troublesome frequencies which filter through, are those at n and $2n/\text{rev}$, respectively. Since the lower harmonics of blade loading are considerably greater than the higher, experience has shown that n/rev vibration of the airframe is the most critical. It can be shown that n/rev fuselage vibrations in the fixed system are a result of the $n-1$, n , and $n+1/\text{rev}$ vibratory response of the blades in the rotating system.

Consider, as an example, a four-bladed rotor. Three factors contribute to the vibratory response: (1) the magnitude of 3, 4, and 5/rev aerodynamic excitation of the blades; (2) the resulting 3, 4, and 5/rev vibratory response of the blades; and (3) the 4/rev coupled response of the airframe or rotor support system.

For a four-bladed helicopter, higher harmonic blade feathering for vibration reduction is achieved by superimposing 4/rev swashplate motion upon basic collective and cyclic flight control inputs. Perturbing the swashplate at 4/rev both vertically and in pitch and roll results in third, fourth, and fifth harmonic blade feathering. Fourth harmonic blade feathering is achieved by oscillating the swashplate vertically about its collective position, while third and fifth harmonic blade feathering results from 4/rev tilting of the swashplate in pitch and roll about its cyclic tilt position.

Since the introduction of the helicopter with its primary means of achieving flight control through first harmonic feathering, engineers have speculated on whether additional advantages could be achieved by higher orders of blade feathering. One of the earliest applications was the work of Drees and Wernicke (Reference 6) who conducted an experimental investigation in 1963 of the effects of second harmonic feathering on the dynamic and aerodynamic characteristics of a modified UH-1A helicopter. The UH-1A

aircraft, with a conventional two-bladed teetering rotor, incorporated a mechanical device by which amplitude and phase of second harmonic feathering were adjustable in flight.

Although the flight test investigation failed to fully achieve its predicted objectives, the project did demonstrate that some reduction in vertical vibration at the aircraft center of gravity could be obtained through proper application of second harmonic feathering. Failure of this work to achieve desired objectives can be attributed to several factors. First, second harmonic feathering strongly couples into both first and third harmonic loads. The first harmonic loads are directly related to those resulting from the basic cyclic pitch required for flight control. Second, it was difficult at best to attempt to introduce higher harmonic control by a mechanical device, open loop, without benefit of feedback.

Following the work of Drees and Wernicke, there have been a number of theoretical and experimental studies directed at further exploring higher harmonic control (References 10 through 14). Continued efforts in this area have been particularly encouraged by the results of experimental work reported by London, Watts, and Sissingh in Appendix C of Reference 1 and summarized by Sissingh and Donham in Reference 2, by the work of Shaw and McHugh reported in References 3 and 4, and most recently by the work of Hammond given in Reference 5. These experimental data indicate in general that successful suppression of vibration can be achieved by oscillating the blade at relatively small amplitudes (in most cases less than 0.5 degree) and that there is negligible effect on alternating blade flapwise and edgewise bending moments. Some increase in blade torsion and corresponding control loads was noted.

3. Wind Tunnel Tests

As already noted, wind tunnel tests of the HHC concept are presently being conducted in the 5-m (16-ft) NASA/Langley TDT. The 2.7-m (9-ft) diameter aeroelastically-scaled model rotor used for the tests is shown installed in the wind tunnel in Figure 2. The sequence of research is outlined in Figure 3, referred to previously.

Dynamic characteristics of the blades are given by the blade frequency diagram presented in Figure 4. The nominal rotor operating speed of 630 rpm represents the rotational speed used for operating the model in Freon-12 for the tests. Observe that edgewise and flapwise modes for the model rotor are representative of full-scale articulated blade values, but in torsion, the model blades are somewhat stiffer than current generation rotors, with the first torsion mode above

9/rev. The blades are 1.3-m (52-in) long with a 10.8-cm (4.24-in) chord. They are restrained by a coincident articulated hinge with its axis offset 7.6-cm (3-in) from the center of rotation. For the model blades, a standard NACA 0012 airfoil was selected, and the blades were untwisted.

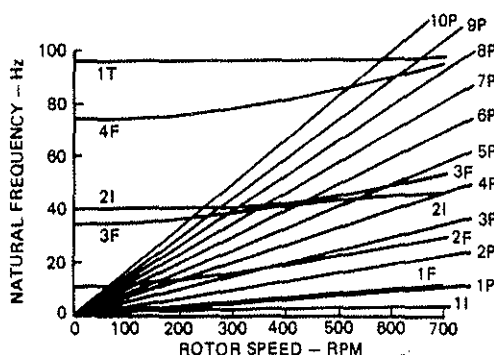


Figure 4. Calculated Model Blade Natural Frequency Characteristics

The first goal of the program was to relate 4/rev vibratory swashplate inputs (collective, pitch, and roll) to 4/rev vibratory forces and moments at the rotor hub. Initial tests were conducted applying manual phase and amplitude sweeps to explore the frequency response of the six hub forces and moments. Fixed system loads were measured by a six-component balance mounted below the model base. Blade and pitch link loads were measured during all tests so as to monitor the influence of higher harmonic control on these parameters.

Figures 5 and 6 help provide a basic understanding of the early tests. Figure 5 illustrates how the 4P hub normal force is affected by a 4P collective input of 0.5 degree at the various phases noted on the figure. The 4P hub normal force response phase and magnitude are given by the azimuthal and radial coordinates respectively of the data points shown. The baseline data point represents the ambient hub 4P normal force response which is to be compensated through the use of higher harmonic feathering. It may be seen from the figure by observing the data point at 27.0 degrees input phase that the 0.5 degree of 4P collective inputs is more than is required to compensate for the baseline response.

Figure 6 is a different presentation of the same data to illustrate how varying the input phase for a constant input amplitude can be used to find the minimum 4P hub response. Once the phase for minimum response is found, the input amplitude can be modulated to obtain the lowest possible 4P hub response. The "optimum" data point on the figure was obtained in this manner.

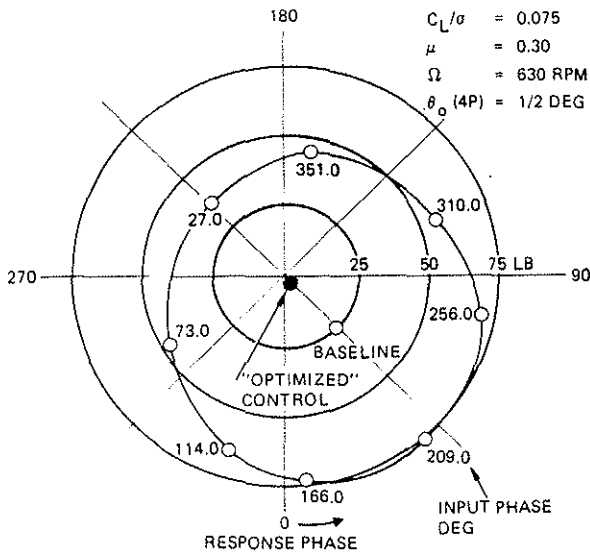


Figure 5. Variation of 4/Rev Normal Force with 4/Rev Collective Input Phase

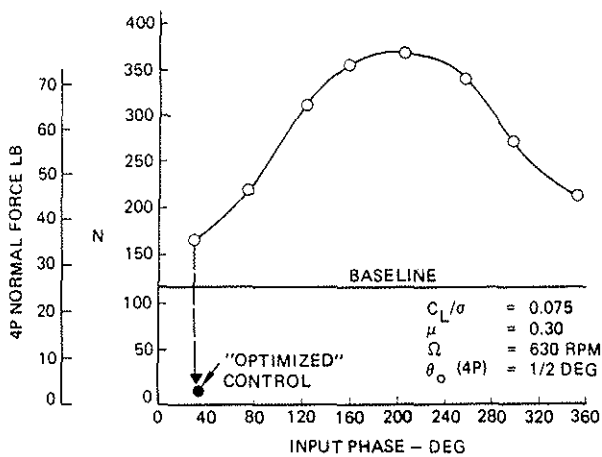


Figure 6. Variation of 4/Rev Normal Force with 4/Rev Collective Input Phase

Wind tunnel results showing the effect of the "optimized" 4P collective input (0.22 degree amplitude, 30 degrees phase) of Figure 6 on blade loads are presented in Figures 7 through 12. Figures 7 and 8 show that the flapwise and edgewise alternating bending moments are relatively insensitive to the 4P input, but Figure 9 indicates that the alternating torsional moment is aggravated. The harmonic decomposition of the root torsional moment shown in Figure 10 indicates that the fourth harmonic component is the primary contributor to this increase in the alternating torsional moment. Figure 11 shows the increase in the fourth harmonic component of torsional moment as a function of radial blade station.

The source of the increase in blade torsional moment is shown vividly in Figure 12 where a harmonic decomposition of the pitch link load is presented. Here it may be noted that, as should be expected, the 4P collective input introduced a significant fourth harmonic response in the pitch link load. As noted in Figure 4 however, the first elastic torsion mode of the blade was above 9P at the design operating speed. Thus, a more torsionally compliant rotor may not have undergone as large amplification in pitch link loading. The increase in 5P content of torsional moment and pitch link load, as depicted in Figures 10 and 12, can be attributed to inadvertent mixing of 4P collective signals with swashplate pitching and rolling motion. Appendix I presents results of a simplified analysis of pitch link loads as a function of 4P feathering. Results indicate that higher harmonic feathering will not induce prohibitive pitch link loads on an OH-6A.

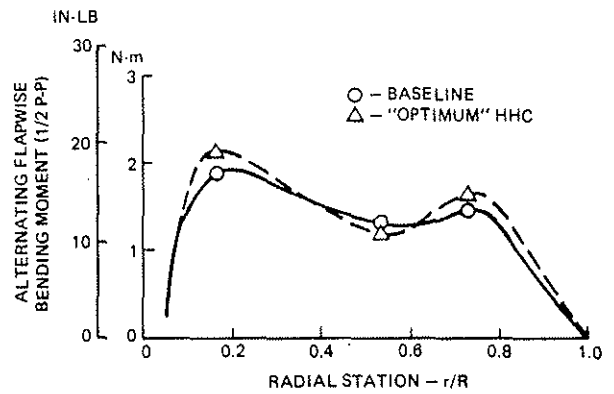


Figure 7. Spanwise Variation of Blade Alternating Flapwise Moment (Ref 5)

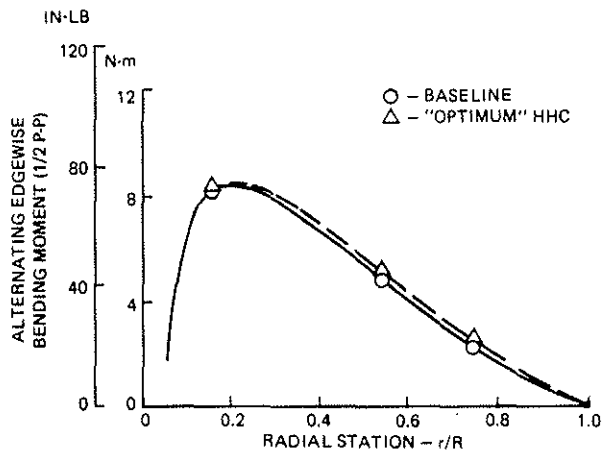


Figure 8. Spanwise Variation of Blade Alternating Edgewise Moment (Ref 5)

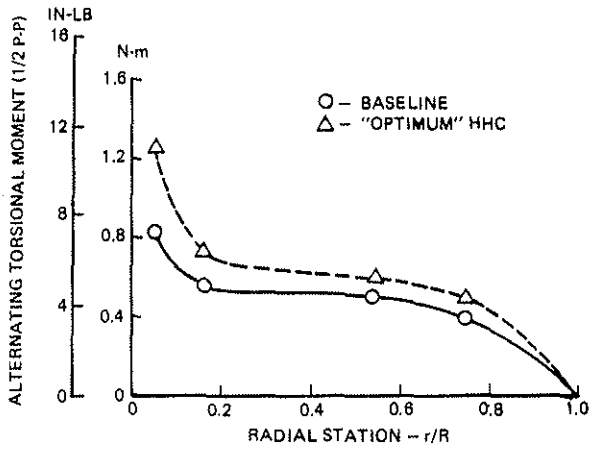


Figure 9. Spanwise Variation of Blade Alternating Torsional Moment (Ref 5)

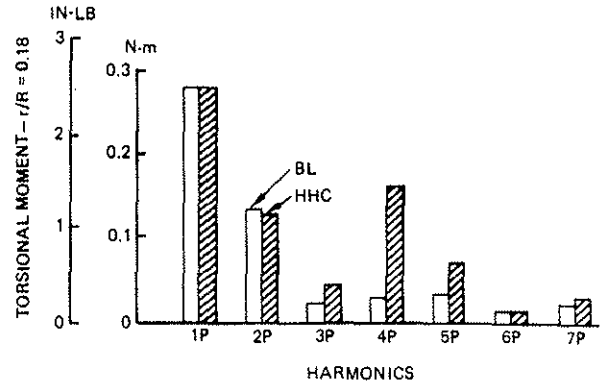


Figure 10. Harmonic Decomposition of Blade Torsional Moment (Ref 5)

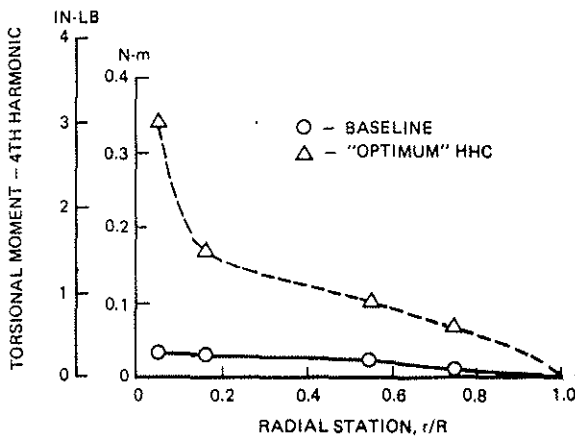


Figure 11. Spanwise Variation of Blade Torsional Moment Fourth Harmonic (Ref 5)

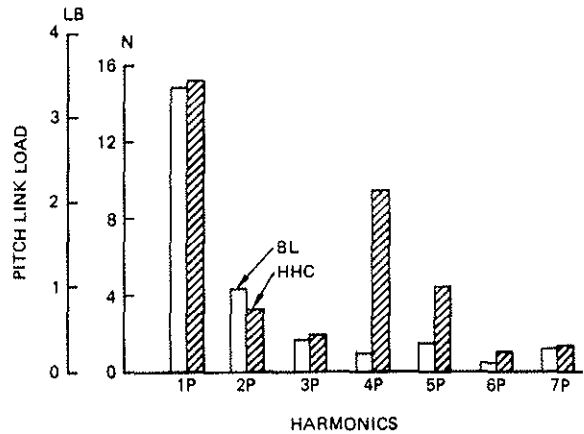


Figure 12. Harmonic Decomposition of Pitch Link Load (Ref 5)

In summary, the wind tunnel tests have shown that by manually sweeping the phase and amplitude of a single 4P input parameter (collective pitch) it is possible to determine the input 4P amplitude and phase sufficient to null a given component of vibratory force (normal force). It should be obvious that such a technique if implemented in an active feedback control system would be highly inefficient. That is, many samplings would have to be made in order to find the correct amplitude and phase of control input to null one component of force.

In actuality, to null vertical fuselage or airframe vibrations it is necessary to minimize not

one component but three components of hub response. Those that primarily contribute to vertical fuselage response are vertical forces, fore-aft forces, and pitching moments. A successful active feedback control system therefore must incorporate solution methods (algorithms) that minimize all three components and that are highly reliable and require a minimum number of samplings. To this end, a number of mathematical methods have been developed. These methods (algorithms) are described in the following section. For illustrative purposes, each algorithm presented will be applied to the wind tunnel test data previously considered (see Figure 5). For reference, those data are given in tabular form in Table I.

TABLE I. SCHEDULE OF 4P COLLECTIVE INPUTS AND HUB RESPONSES

$\mu = 0.30, C_L/\sigma = 0.075$

Higher Harmonic Blade Feathering for Helicopter Vibration Reduction

Phase/Amplitude Notation

Input	Response of Interest	4P Input Amp (deg)	4P Input Phase (deg)	4P Total Output Amp N (lb)	4P Output Phase (deg)
213	Baseline/Normal Force	0.00	0.0	114.8 (25.4)	44.0
214	Collective/Normal Force	0.50	27.0	157.5 (35.4)	-138.0
215	Collective/Normal Force	0.50	75.0	207.3 (46.6)	-59.0
216	Collective/Normal Force	0.49	114.0	259.1 (58.0)	-26.0
217	Collective/Normal Force	0.49	166.0	328.7 (73.9)	13.0
218	Collective/Normal Force	0.49	-191.0	399.8 (89.4)	41.0
219	Collective/Normal Force	0.48	-104.0	315.4 (70.9)	75.0
220	Collective/Normal Force	0.49	-50.0	254.0 (57.1)	121.0
221	Collective/Normal Force	0.49	-9.0	200.2 (45.0)	165.0
optimal	Collective/Normal Force	0.22	0.0	2.0	42.0

4. Harmonic Control Solution Algorithms

The effectiveness of higher harmonic control having been established through wind tunnel testing described in the previous section, algorithms for solving for required feathering inputs are developed next. The need to implement higher harmonic control in an adaptive control system places special requirements on solution techniques. Algorithms to be employed must be numerically efficient to permit a high solution update rate. It follows that the algorithm must require a minimum of sampled data, both in quantity and type to avoid burdensome data acquisition requirements. Finally, there exist several control modes that must be explored, such that an optimal control input solution can be derived. These control modes are:

- A single swashplate degree of freedom (pitch, roll, collective) is used to control a single hub response.

- A single swashplate degree of freedom is used to control an aggregate of hub responses.
- Multiple swashplate degrees of freedom are used to control a single hub response.
- Multiple swashplate degrees of freedom are used to control multiple hub responses.

Solution techniques have currently been derived for the single-input/single-output and multiple-input/multiple-output modes of harmonic control. The algorithms are presented in the sections that follow.

Single-Input/Single-Output Solution Algorithms

Several solution techniques have been developed to calculate 4P phase and amplitude of a single swashplate input necessary to suppress a single transmitted hub response. These techniques were developed in support of a 1977 NASA/Langley TDT test program and, consequently, results have been generated from available test data. The various techniques will be developed and contrasted in the following section.

Three-Point Technique

In developing numerical algorithms to calculate optimal swashplate inputs, advantage was taken of the almost linear relationship between 4P feathering inputs and 4P hub oscillatory forces and moments. The first such approach developed requires advanced knowledge of baseline vibration levels and two samples of oscillatory output in response to known 4P feathering inputs. By using 4P collective swashplate inputs to minimize 4P hub normal forces, the procedure can be outlined as follows:

1. Define feathering inputs and response quantities as phasors having magnitude and phase as:

$$\bar{F}_{ZBL} = (|\bar{F}_{ZBL}|, \phi_{ZBL})$$

Phasor representing 4P component of baseline hub normal force, with amplitude $|\bar{F}_{ZBL}|$ and phase relative to an index blade ϕ_{ZBL}

$$\bar{F}_{Z1} = (|\bar{F}_{Z1}|, \phi_{Z1})$$

Phasor representing 4P component of hub normal force in response to an arbitrary 4P collective input

$$\bar{F}_{Z2} = (|\bar{F}_{Z2}|, \phi_{Z2})$$

Phasor representing 4P component of hub normal force in response to an arbitrary 4P collective input different from above

$$\bar{\theta}_{01} = (|\bar{\theta}_{01}|, \Delta\phi_{01})$$

Phasor representing the first arbitrary 4P collective perturbation with magnitude $|\bar{\theta}_{01}|$ and phase $\Delta\phi_{01}$

$$\bar{\theta}_{02} = (|\bar{\theta}_{02}|, \Delta\phi_{02})$$

Phasor representing a second arbitrary 4P collective perturbation

2. Transform phase and amplitude to sine and cosine magnitudes:

$$F_{ZCBL} = |\bar{F}_{ZBL}| \cos \phi_{ZBL}$$

$$F_{ZSBL} = |\bar{F}_{ZBL}| \sin \phi_{ZBL}$$

$$\theta_{OC1} = |\bar{\theta}_{01}| \cos \Delta\phi_{01}$$

$$\theta_{OS1} = |\bar{\theta}_{01}| \sin \Delta\phi_{01}$$

⋮
etc.

3. Assume there exists a plane, Figure 13, that describes the relationship between 4P hub normal force cosine magnitude and 4P swashplate collective sine and cosine magnitudes. Assume a similar plane exists for the sine magnitude of 4P hub normal force. In addition, establish the following limitations:

- a. The F_{ZC} and F_{ZS} planes are not parallel to each other
 - b. Neither of the two planes are parallel to the plane of zero response ($F_{ZC} = F_{ZS} = 0$)
 - c. The locus of points representing the intersection of the planes is not parallel to the plane of zero response.
4. Write equations for the F_{ZC} and F_{ZS} planes in terms of two arbitrary coefficients and baseline magnitudes.

$$A^{\theta}_{OC} + B^{\theta}_{OS} + (F_{ZC} - F_{ZCBL}) = 0 \quad (1)$$

$$D^{\theta}_{OC} + E^{\theta}_{OS} + (F_{ZS} - F_{ZSBL}) = 0 \quad (2)$$

By substituting two frequency response samples, the coefficients in Equations (1) and (2) may be determined.

5. Referring to Figure 13, F_{ZC} and F_{ZS} in Equations (1) and (2), respectively, may now be set to zero. This yields equations for two lines in the zero-response plane, represented by line segments AB and CD in Figure 13. Simultaneous solution of the two equations yields point P, whose coordinates are the sine and cosine magnitudes of the 4P collective input needed to null the sine and cosine magnitudes of hub response.

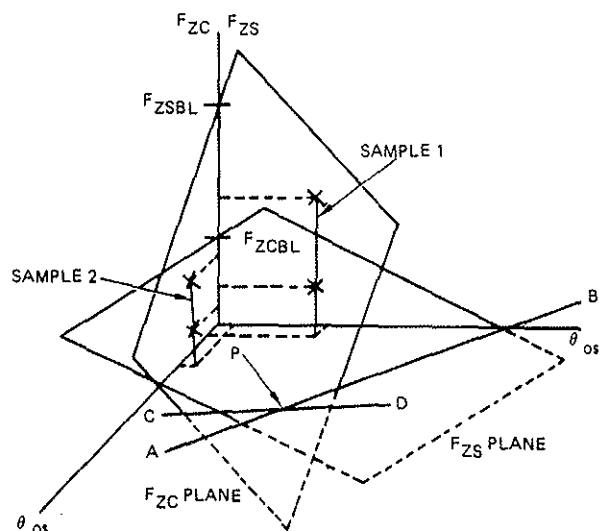


Figure 13. Planar Relationships Between 4P Collective Input and 4P Shaft Axial Force Sin and Cos Components

A schedule of 4P collective inputs and resulting 4P hub normal force responses for a particular wind tunnel trim condition is presented in Table I. The test was conducted such that 4P collective amplitude was held constant while phase was swept manually in near 45-degree increments. Table II presents results using data from Table I with the three-point technique. Results were calculated based on combinatorial permutations of two of the eight available data points to check solution consistency. A single solution was then obtained by neglecting those solutions with phase greater than one standard deviation away from the mean phase. A new mean phase and amplitude were then calculated from the reduced set of solutions. Results generated from test data were fairly consistent with three exceptions noted in Table II. Close examination revealed that when 4P perturbations were made 180 degrees apart, as were the three flagged cases of Table II, the

planes that resulted were vertical and coplanar, thereby defining an infinite set of non-unique solutions. Rather than impose a sampling scheme to preclude 180-degree-apart sampling, it was deemed more appropriate to develop a technique that has no such constraints.

TABLE II. SOLUTION INPUTS BASED ON THREE-POINT TECHNIQUE (DATA FROM TABLE I)

Three-Point Higher Harmonic Solution

Data from Cases		4P Input Amplitude	4P Input Phase
214	215	0.2115	28.1005
214	216	0.2109	28.1328
214	217	0.2100	28.2249
214	218	0.1974	26.1319
214	219	0.2113	28.3749
214	220	0.2109	28.2207
214	221	0.2109	28.0845
215	216	0.2519	26.2867
215	217	0.2510	25.2689
215	218	0.2511	32.3555
215	219	0.3616	91.0183
215	220	0.2413	23.0785
215	221	0.2236	28.4521
216	217	0.2505	24.5436
216	218	0.2512	32.7101
216	219	0.2416	40.1010
216	220	0.2186	13.6416
216	221	0.2081	29.9136
217	218	0.2515	33.4378
217	219	0.2442	31.5965
217	220	0.2649	28.0025
217	221	0.1028	87.1869
218	219	0.2504	33.1809
218	220	0.2522	33.0913
218	221	0.2562	32.9755
219	220	0.2316	34.1967
219	221	0.2208	34.3967
220	221	0.2083	34.6520
Linear Higher Harmonic Solution			
4P Input Amplitude		4P Input Phase	
0.2325		30.1404	

Nonlinear (Six-Point) Technique

The second numerical approach investigated replaces the planes of the former approach with second-order surfaces defined by Equations (3) and (4):

$$A\theta_{OC}^2 + B\theta_{OS}^2 + C\theta_{OC}\theta_{OS} + D\theta_{OC} + E\theta_{OS} = F_{ZC} - F_{ZCBL} \quad (3)$$

$$F\theta_{OC}^2 + G\theta_{OS}^2 + H\theta_{OC}\theta_{OS} + I\theta_{OC} + J\theta_{OS} = F_{ZS} - F_{ZSBL} \quad (4)$$

The shape functions above are similar to cubic polynomials used in finite element plate analysis; the lower-order terms are retained to improve the approximation while higher-order terms are eliminated to reduce the number of samples required to define coefficients A through J.

In addition to a baseline condition, five sample swashplate inputs and resulting hub responses are required to uniquely define the two shape functions. Once the ten coefficients are defined, a Newton-Raphson iterative scheme is used to solve the set of nonlinear algebraic equations for the required swashplate inputs.

Table III presents results generated from Table I data using the nonlinear approach. Good agreement is seen between the linear and nonlinear algorithms, indicating hub forces are more linear than nonlinear with control inputs of small amplitude.

The paramount drawback to this type of analysis lies in its arduous data processing requirements. The inversion of 5 by 5 matrices coupled with an iterative solution process could erode control loop response. Thus, a third predictive analysis was investigated which has no inherent sampling constraints nor exhaustive data processing requirements.

TABLE III. SOLUTION INPUT BASED ON SIX-POINT NONLINEAR TECHNIQUE (DATA FROM TABLE I)

Nonlinear Higher Harmonic Solution
Using Newton-Raphson Iteration

Number of Iterations = 3

Data from Cases	4P Input Amplitude	4P Input Phase
214, 215, 216, 217, 218	0.2230	29.5149

Two-Point Technique

The third single-input/single-output algorithm investigated requires a baseline and only one sample swashplate input and resulting hub frequency response to provide a solution. The technique is based on the following tacit assumption: if higher harmonic partial response is defined as that portion of hub oscillatory force due solely to 4P feathering inputs (i. e., total response minus baseline response), then 4P sample input phase leads harmonic partial response phase by a constant amount. The validity of this assumption using Table I data is

established in Table IV. Referring to Figure 14, the algorithm can be summarized as follows:

1. Using phasor notation, vectorially subtract the baseline hub response of interest from the perturbation hub response.

$$\bar{F}_{ZHH} = \bar{F}_{Z1} - \bar{F}_{ZBL} \quad (5)$$

2. Rotate the higher harmonic partial response phasor until it opposes the baseline phasor. If \bar{F}_{ZHH} has magnitude and phase $|\bar{F}_{ZHH}|$ and θ_{ZHH} , respectively, this step requires a rotation of magnitude $\theta_{ZHH} - (\phi_{ZBL} - 180)$.
3. By virtue of the assumption that the difference between control input phase and harmonic control partial response phase is constant for a given flight condition, the required control input phase may be written

$$\Delta\phi_c = \Delta\phi_{c1} - (\theta_{ZHH} - (\phi_{ZBL} - 180)) \quad (6)$$

4. Allowing that harmonic control partial response magnitude $|\bar{F}_{ZHH}|$ is linear with control input amplitude, the required control input amplitude for nulling baseline response is

$$|\bar{u}_c| = |\bar{u}_{c1}| \frac{|\bar{F}_{ZBL}|}{|\bar{F}_{ZHH}|} \quad (7)$$

TABLE IV. ASSUMPTION: SAMPLE INPUT PHASE LEADS HIGHER HARMONIC CONTROL PARTIAL RESPONSE PHASE BY CONSTANT AMOUNT

4P Collective Input Phase (deg)	4P HHC Partial Response Phase	Δ
27	222	196
73	275	202
114	310	197
166	358	193
209	39	190
256	90	194
310	147	197
351	185	194

Table V presents results generated by the two-point approach using wind tunnel data from Table I. The level of agreement between this approach and the previous techniques indicates it is the most likely candidate for control applications, given its generality and simplicity.

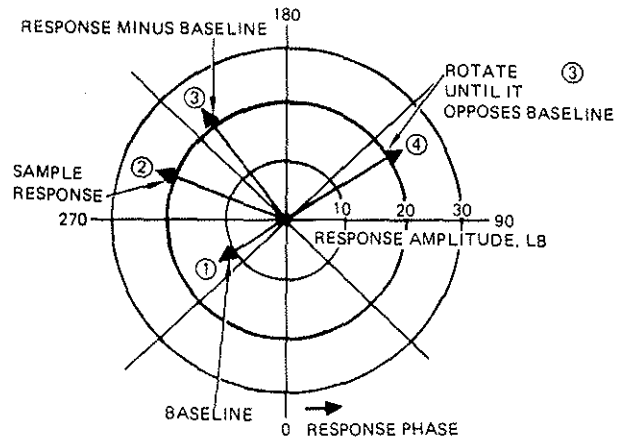


Figure 14. Two-Point Higher Harmonic Solution Technique

TABLE V. SOLUTION INPUTS BASED ON TWO-POINT TECHNIQUE (DATA FROM TABLE II)

Two-Point Higher Harmonic Solution

Data from Case	4P Input Amplitude	4P Input Phase
214	0.2108	28.1569
215	0.2219	21.6276
216	0.2066	27.3438
217	0.2365	31.3915
218	0.2496	33.5275
219	0.2449	29.7635
220	0.2213	26.8919
221	0.2028	29.2229
Linear Higher Harmonic Solution		
4P Input Amplitude	4P Input Phase	
0.2205	28.7951	

Thus, it has been established that by virtue of the almost linear relationship between feathering inputs and hub oscillatory forces, several techniques exist for predicting 4P control input to minimize baseline vibrations on the basis of sampled data. The potential of these techniques, as well as others to be applied in a multiple-input/multiple-output mode, will be discussed in the next section.

5. Multiple-Input/Multiple-Output Harmonic Control

A primary consideration in approaching higher harmonic control in a multiple-input/multiple-output mode is that there exist only three independent swashplate degrees of freedom to minimize six hub vibratory responses. One approach is to minimize just the three hub responses that largely contribute to vertical fuselage response; namely, 4/rev vertical forces, 4/rev fore-aft forces and 4/rev pitching moments at the hub. Alternatively, one could address the responses contributing to lateral fuselage response: 4/rev side forces and 4/rev rolling and yawing moments, or some combination of the two.

Techniques developed for calculating optimal swashplate inputs for suppressing multiple hub responses all assume the same general linear relationship between 4P hub responses and 4P feathering inputs. Consider the vertical vibration problem, for example:

$$\left. \begin{aligned} \Delta \bar{F}_Z &= \frac{\partial \bar{F}_Z}{\partial Z} \delta Z + \frac{\partial \bar{F}_Z}{\partial \theta} \delta \theta + \frac{\partial \bar{F}_Z}{\partial \phi} \delta \phi \\ \Delta \bar{M}_{YY} &= \frac{\partial \bar{M}_{YY}}{\partial Z} \delta Z + \frac{\partial \bar{M}_{YY}}{\partial \theta} \delta \theta + \frac{\partial \bar{M}_{YY}}{\partial \phi} \delta \phi \\ \Delta \bar{F}_X &= \frac{\partial \bar{F}_X}{\partial Z} \delta Z + \frac{\partial \bar{F}_X}{\partial \theta} \delta \theta + \frac{\partial \bar{F}_X}{\partial \phi} \delta \phi \end{aligned} \right\} (8)$$

or the lateral-torsion vibration problem

$$\left. \begin{aligned} \Delta \bar{F}_Y &= \frac{\partial \bar{F}_Y}{\partial Z} \delta Z + \frac{\partial \bar{F}_Y}{\partial \theta} \delta \theta + \frac{\partial \bar{F}_Y}{\partial \phi} \delta \phi \\ \Delta \bar{M}_{XX} &= \frac{\partial \bar{M}_{XX}}{\partial Z} \delta Z + \frac{\partial \bar{M}_{XX}}{\partial \theta} \delta \theta + \frac{\partial \bar{M}_{XX}}{\partial \phi} \delta \phi \\ \Delta \bar{M}_{ZZ} &= \frac{\partial \bar{M}_{ZZ}}{\partial Z} \delta Z + \frac{\partial \bar{M}_{ZZ}}{\partial \theta} \delta \theta + \frac{\partial \bar{M}_{ZZ}}{\partial \phi} \delta \phi \end{aligned} \right\} (9)$$

In matrix notation,

$$\begin{Bmatrix} \Delta \bar{F}_Z \\ \Delta \bar{M}_{YY} \\ \Delta \bar{F}_X \end{Bmatrix} = [H_1] \begin{Bmatrix} \delta Z \\ \delta \theta \\ \delta \phi \end{Bmatrix}; \quad \begin{Bmatrix} \Delta \bar{F}_Y \\ \Delta \bar{M}_{XX} \\ \Delta \bar{M}_{ZZ} \end{Bmatrix} = [H_2] \begin{Bmatrix} \delta Z \\ \delta \theta \\ \delta \phi \end{Bmatrix} \quad (10)$$

It is seen that the transfer matrices relating 4P swashplate inputs to 4P hub oscillatory responses are fully coupled. Preliminary test data have shown that optimal swashplate inputs for the multiple-input case are not simply a linear combination of optimal inputs for the respective single-input cases. Thus, interharmonic coupling must be adequately represented in the analytical model.

Using measured normal force, axial force and pitching moment hub frequency response data (of which Table I is a subset), the transfer matrix $[H_1]$ was calculated and inverted. Solution of the coupled equations yielded the following swashplate multiple inputs to null vibration:

Collective:	0.15-degree amplitude 302-degree phase
Lateral Cyclic:	0.69-degree amplitude 129-degree phase
Longitudinal Cyclic:	0.60-degree amplitude 92-degree phase

It is interesting to note that not only are the optimal pitch angles of reasonable magnitude, but the collective input required has decreased from that of the single-input case (0.22 degrees).

In developing a technique for generating the necessary transfer matrices, it is desirable to again minimize sampling and data processing requirements. Thus, to simply extend the six-point nonlinear technique to three inputs and three outputs, would require fifteen input perturbations, and forty-eight Fast Fourier Transform (FFT) spectral analyses to derive elements of the transfer matrix, thereby proving too burdensome for adaptive control systems. Similarly, the three-point technique would require six input perturbations and 21 FFTs in a three-input, three-output mode. Even extending the two-point technique to such a mode would require three perturbations and twelve FFTs per solution update. A multiple linear regression technique, outlined in Reference 15, requires only three perturbations and six FFTs, thereby representing an attractive approach to multiple-input/multiple-output higher harmonic control.

Multiple Regression Solution Technique

The analysis of a linear system with p inputs and a single output shall be considered first. The assumption of linearity dictates that a single hub response (e.g., normal force) can be written in terms of individual component

responses to the p inputs, (swashplate pitch, roll, collective) as follows:

$$F_z(t) = F_{z_1}(t) + F_{z_2}(t) + F_{z_3}(t) + F_{z_0}(t) \quad (11)$$

where F_{z_0} represents baseline normal force response. Writing DuHamel's integral for the individual inputs, then taking Fourier transforms and summing yields the frequency domain counterpart of Equation (11).

$$F_z(f) = \sum_{k=1}^p H_{kF_z}(f) X_k(f) + F_{z_0}(f) \quad (12)$$

Acknowledging the existence of additive random noise, the p transfer coefficients $H_{kF_z}(f)$ are calculated (References 15 and 16) by writing the probability density function for noise in terms of these coefficients and maximizing the probability estimate.

$$\begin{bmatrix} \hat{H}_{1F_z} \\ \hat{H}_{2F_z} \\ \vdots \\ \hat{H}_{pF_z} \end{bmatrix} = D^{-1} \begin{bmatrix} (\bar{F}_z, X_1) \\ (\bar{F}_z, X_2) \\ \vdots \\ (\bar{F}_z, X_p) \end{bmatrix} \quad (13)$$

where

$$D = \begin{bmatrix} (X_1, X_1) & (X_2, X_1) & \dots & (X_p, X_1) \\ (X_1, X_2) & (X_2, X_2) & \dots & (X_p, X_2) \\ \vdots & \vdots & \ddots & \vdots \\ (X_1, X_p) & (X_2, X_p) & \dots & (X_p, X_p) \end{bmatrix} \quad (14)$$

and the inner products are defined by

$$(X_j, X_l) = \sum_{v=1}^N X_{jv} X_{lv}^* \quad (15)$$

$(j, l = 1, 2, \dots, p) \quad N \geq p$

where in this case ()^{*} denotes complex conjugate. In addition,

X_{1v} = Complex Fourier transform of swashplate collective inputs at frequency f_v

X_{2v} = Complex Fourier transform of swashplate lateral cyclic inputs at frequency f_v

X_{3v} = Complex Fourier transform of swashplate longitudinal cyclic inputs at frequency f_v

If the above analysis is performed two more times, one each for hub pitching moment and axial force, we obtain

$$\begin{bmatrix} \hat{H}_{F_z} \\ \hat{H}_{M_y} \\ \hat{H}_{F_x} \end{bmatrix} = D^{-1} \begin{bmatrix} (\bar{F}_z, X_1) & (\bar{M}_y, X_1) & (\bar{F}_x, X_1) \\ (\bar{F}_z, X_2) & (\bar{M}_y, X_2) & (\bar{F}_x, X_2) \\ (\bar{F}_z, X_3) & (\bar{M}_y, X_3) & (\bar{F}_x, X_3) \end{bmatrix} \quad (16)$$

$(3 \times 3) \quad (3 \times 3) \quad (3 \times 3)$

Thus, Equation (12) can be extended to include three hub outputs as follows:

$$\begin{bmatrix} \bar{F}_z(f) - F_{z_0}(f) \\ \bar{M}_y(f) - M_{y_0}(f) \\ \bar{F}_x(f) - F_{x_0}(f) \end{bmatrix} = \begin{bmatrix} H_{F_z} \\ H_{M_y} \\ H_{F_x} \end{bmatrix} \begin{bmatrix} X_1(f) \\ X_2(f) \\ X_3(f) \end{bmatrix} \quad (17)$$

The higher harmonic solution input is obtained by setting \bar{F}_z , \bar{M}_y and \bar{F}_x to zero, inverting the complex transfer function matrix and multiplying:

$$\begin{bmatrix} X_1(f) \\ X_2(f) \\ X_3(f) \end{bmatrix}^* = \begin{bmatrix} H_{F_z} \\ H_{M_y} \\ H_{F_x} \end{bmatrix}^{-1} \begin{bmatrix} -F_{z_0}(f) \\ -M_{y_0}(f) \\ -F_{x_0}(f) \end{bmatrix} \quad (18)$$

where * now denotes an optimal solution.

It is seen that the transfer function generated in this estimation technique can be used to relate 3, 4, and 5/rev harmonic blade pitching to similar harmonics of blade flapwise and edgewise root shears. Writing third, fourth, and fifth harmonic blade pitching in terms of fourth harmonic swashplate pitching, rolling and collective motion in addition to solving for similar harmonics of blade root shears in terms of fourth harmonic hub forces and moments permits the direct application of Equation (18). Once an objective function

is written in terms of swashplate displacements and hub forces and moments, optimal swashplate inputs required to null certain hub vibratory forces can be derived, as in Equation (18). Reference 16 presents details for the construction of a confidence region for the estimate of the frequency response function at a given frequency. In addition, special smoothing and filtering techniques may be necessary to improve the statistical nature of the sampled data. Reference 9 lists several frequency domain techniques for smoothing raw spectra.

6. Features of a Flightworthy Active Control System

The final step in the current higher harmonic control program is the demonstration of a flightworthy active control system. Elements of a typical active vibration suppression system are illustrated in Figures 15 and 16. For the OH-6A shown, vibratory forces and moments are sensed by a strain-gauge array mounted on the helicopter's static (nonrotating) mast. Hughes Helicopters' designs incorporate a nonrotating mast which houses the main rotor drive shaft. Thus, all rotor loads (except torsion) are transmitted to the fuselage through the mast, thereby facilitating the task of obtaining rotor feedback. Strain-gauge data are then fed to a microprocessor located in the cabin.

Once obtained, the strain-gauge data is digitized and an optimal solution determined by means of an onboard, general purpose digital microprocessor. Digital-to-analog conversion yields voltages proportional to optimal 4P phase and amplitude for each of three actuators. These are input to an oscillator that generates corrective 4P sinusoidal signals which drive the high-frequency electrohydraulic actuators. During initial flight testing, blade and pitch link loads will be monitored to ensure that such loads remain within allowable fatigue limits. The sequence of control flow is illustrated in Figure 17.

Once initial input parameters have been loaded either on the ground or in flight from an external storage device, baseline hub vibratory response levels are obtained. The 4P spectral content is calculated and stored for each hub force degree of freedom. Following a 4P perturbation of the swashplate, hub 4P response is again determined and stored. Phase and amplitude of the 4P inputs is obtained from a servo ram linear variable differential transformer (LVDT) and input to a hub response analysis. Calculated hub response is compared with actual response data and optimal 4P phases and amplitudes calculated from the error and baseline response data. Although the active control system under consideration features three channels

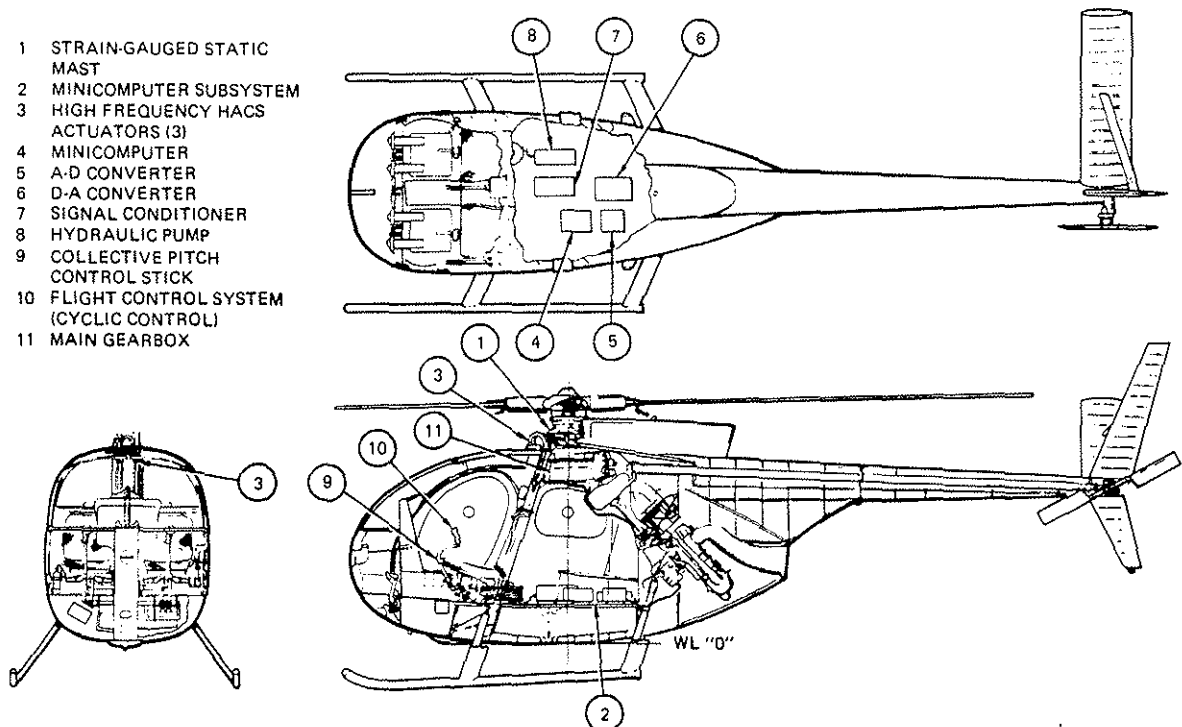


Figure 15. OH-6A Installation of Active Higher Harmonic Control System

of hub vibratory response and inputs, Figure 17 illustrates a single channel case.

Active system design criteria should be addressed as early as possible in the design cycle so as to take advantage of the opportunity to integrate the system with existing control concepts. Thus if more than one control concept is implemented, such as a stability augmentation system, (SAS), there may be benefits in utilizing common system components. Also, close attention should be paid to fail operational characteristics of the system. Reliability criteria include the following:

- With an in-flight failure, the HHC system reverts to the primary control system.
- The HHC system must incorporate a stable control loop sequence.
- A manual pilot override should be provided to be used for a failure in the microprocessor.
- The HHC system should be designed to monitor pitch link loads with an automatic cutout, should these exceed limit load.

With reliability and safety of flight requirements established, design criteria for hydraulic, electrical, and cooling subsystems can be determined. That is, once frequency and amplitude limits for higher harmonic feathering are established, this defines hydraulic flow rates and corresponding hydraulic system power and cooling requirements.

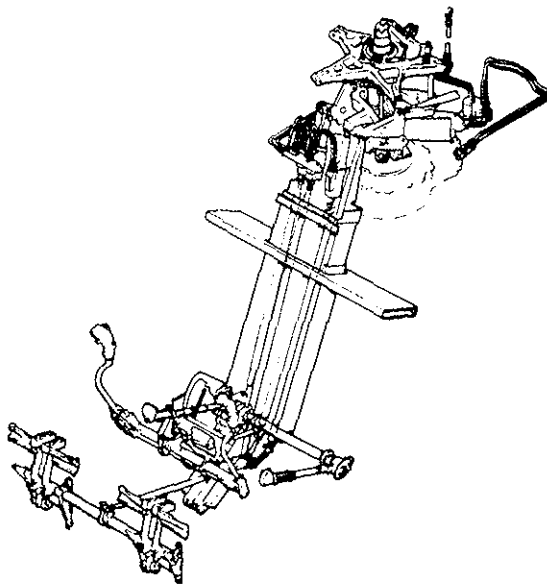


Figure 16. OH-6A Higher Harmonic Control System Actuator Installation

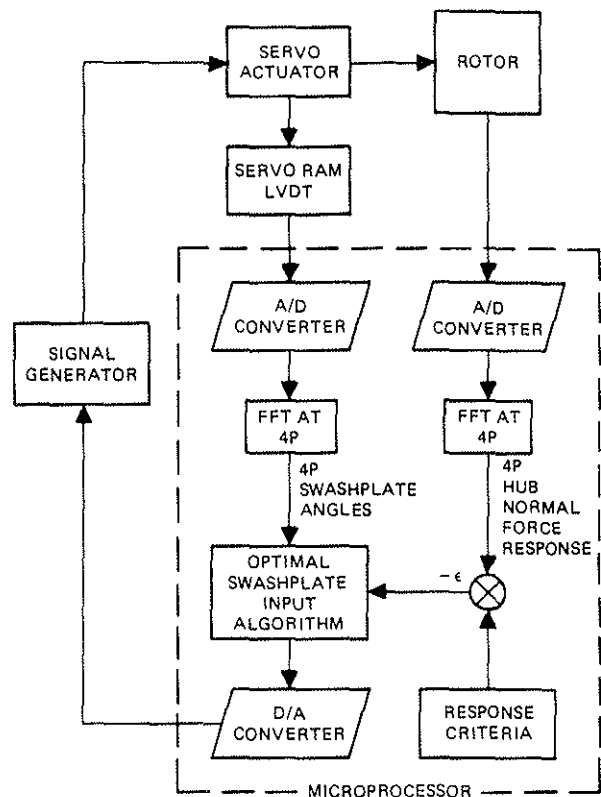


Figure 17. Active Vibration Suppression System Control Flow

7. Conclusions

Data obtained from a recent wind tunnel investigation of single-input/single-output higher harmonic control have led to the following conclusions:

- By varying phase and amplitude of higher harmonic blade feathering, the 4P spectral components of hub oscillatory responses can be minimized for a given trim condition.
- For the model rotor tested, 4P collective inputs needed to minimize 4P hub normal forces induced higher peak-to-peak torsional moments and, hence, higher pitch link loads on an articulated rotor.
- Flapwise and chordwise bending moments were fairly insensitive to "optimal" 4P collective inputs, on the rotor tested.

An investigation of several techniques for predicting 4P swashplate inputs needed to minimize 4P hub vibratory responses using wind

tunnel test data has generated the following conclusions:

- There exists an almost linear relationship between 4P hub responses and 4P feathering inputs.
- Optimal single inputs can be generated from vibratory response data. Such inputs can be calculated from a completely general six-point nonlinear algorithm. However, by taking advantage of several key assumptions, a computationally more efficient technique can be derived requiring only two sample response data points.
- Techniques exist for treating the multiple-input/multiple-output mode of higher harmonic control. The effectiveness of these algorithms will be assessed in an upcoming wind tunnel program.

REFERENCES

1. R.J. London, G.A. Watts, and G.J. Sissingh, Experimental Hingeless Rotor Characteristics at Low Advance Ratio with Thrust, NASA CR-114684, December 1973.
2. G.J. Sissingh and R.E. Donham, Hingeless Rotor Theory and Experiment on Vibration Reduction by Periodic Variation of Conventional Controls, Rotorcraft Dynamics, NASA SP-352, February 1974.
3. F.J. McHugh and J. Shaw, Jr., Benefits of Higher-Harmonic Blade Pitch: Vibration Reduction, Blade-Load Reduction and Performance Improvement, Proceedings of the American Helicopter Society Mideast Region Symposium on Rotor Technology, August 1976.
4. F.J. McHugh and J. Shaw, Jr., Helicopter Vibration Reduction with Higher Harmonic Blade Pitch, Proceedings of the Third European Rotorcraft and Powered-Lift Aircraft Forum, Paper No. 22, September 1977.
5. C.E. Hammond, Helicopter Vibration Reduction Via Higher Harmonic Control, Structures Laboratory, U.S. Army Research and Technology Laboratories, Proceedings of the Rotorcraft Vibration Workshop, NASA Ames Research Center, February 22-23, 1978.
6. R.K. Wernicke and J.M. Drees, Second Harmonic Control, Proceedings of the American Helicopter Society, 19th Annual National Forum, Washington, D.C., May 1-3, 1963.
7. J.W. Cooley and J.W. Tukey, an Algorithm for the Machine Calculation of Complex Fourier Series, Mathematical Computation, Vol. 19, pp. 297-301, April 1965.
8. E.O. Brigham, The Fast Fourier Transform, Prentice Hall, Inc., New Jersey, 1974.
9. R.K. Otnes and L. Enochson, Digital Time Series Analysis, John Wiley & Sons, Inc., New York, 1972.
10. H. Daughaday, Suppression of Transmitted Harmonic Rotor Loads by Blade Pitch Control, USAAVLABS Technical Report 67-14, November 1967. Also see Proceedings of the American Helicopter Society, 23rd Annual National Forum, Washington, D.C., May 10-12, 1967.
11. J.C. Balcerak and J.C. Erickson, Jr., Suppression of Transmitted Harmonic Vertical and Inplane Rotor Loads by Blade Pitch Control, USAAVLABS Technical Report 69-39, July 1969.
12. J. Shaw, Higher Harmonic Blade Pitch Control for Helicopter Vibration Reduction: A Feasibility Study, MIT Report ASRL TR 150-1, December 1968.
13. R.M. Williams and E.O. Rogers, Design Considerations of Circulation Control Rotors, Proceedings of the 28th Annual Forum of the American Helicopter Society, May 1972.
14. J.L. McCloud, III, and M. Kretz, Multicyclic Jet-Flap Control for Alleviation of Helicopter Blade Stresses and Fuselage Vibrations, Rotorcraft Dynamics, NASA SP-352, February 1974.
15. R.W. Powers, Application of Higher Harmonic Blade Feathering for Helicopter Vibration Reduction, NASA Interim Technical Report, Contract NAS1-14552, * Hughes Helicopters, Culver City, CA, April 1978.
16. H. Akaike, On the Statistical Estimation of the Frequency Response Function of a System Having Multiple Input, Annals of the Institute of Statistical Mathematics, Vol. 17, No. 2.
17. C.E. Hammond and W.H. Weller, Recent Experience in the Testing of a Generalized Rotor Aeroelastic Model at Langley Research Center, Proceedings of the Second European Rotorcraft and Powered Lift Aircraft Forum, Buckeburg, Federal Republic of Germany, September 20-22, 1976, Paper 35.

*Copies of this report may be obtained by writing the author at Hughes Helicopters, Culver City, CA, 90230.

APPENDIX I
CONTROL LOADS

As noted previously, 4P response of the model pitch link loads during harmonic feathering was notably degraded. Although tennis racket-type torsional loading as induced by high frequency blade feathering tends to aggravate control loads, it is apparent that such loads may fall within present design criteria in most applications. Consider the rigid blade, rigid pitch link approximation to a feathering rotor in Figure I. 1. The feathering equation of motion for such a rigid system in a vacuum can be written as,

$$(I_{zz} + I_{yy}) \ddot{\phi}(t) + \Omega^2 \phi(t) (I_{zz} - I_{yy}) = RP(t) \quad (I. 1)$$

where I_{zz} and I_{yy} are blade cross section chordwise and flapwise mass moments of inertia, and R is the pitch-link/feathering-axis offset.

Since

$$I_{zz} \gg I_{yy}$$

in most cases we can write

$$(I_{zz} + I_{yy}) \approx (I_{zz} - I_{yy}) \approx I_{xx} \quad (I. 2)$$

where I_{xx} is the blade feathering inertia.

By imposing simple harmonic motion as follows,

$$\phi(t) = A \sin(4\Omega t + \theta) \quad (I. 3)$$

$$P(t) = P_o \sin(4\Omega t + \theta) \quad (I. 4)$$

and substituting equations (I. 2), (I. 3), and (I. 4) into (I. 1), the following relation for 4P control load amplitude in terms of 4P feathering amplitude can be derived:

$$P_o = 15 \frac{\Omega^2 A I_{xx}}{R} \quad (I. 5)$$

Table I. 1 presents pertinent configuration data for the nine-foot wind tunnel model rotor as well as OH-6A blade data. Calculated 4P pitch link load amplitude under the influence of 0.22-degree 4P feathering is presented for both blades.

The ability of equation (I. 1) to predict 4P control loads is substantiated in Figure I. 1. The corresponding 10.1-lbf penalty associated with

4P pitching of an OH-6A blade is not prohibitive and easily falls within current design criteria for standard pitch links. Since the control load penalty is a function of the square of feathering frequency, critical attention should be given to control loads in higher frequency applications of harmonic feathering.

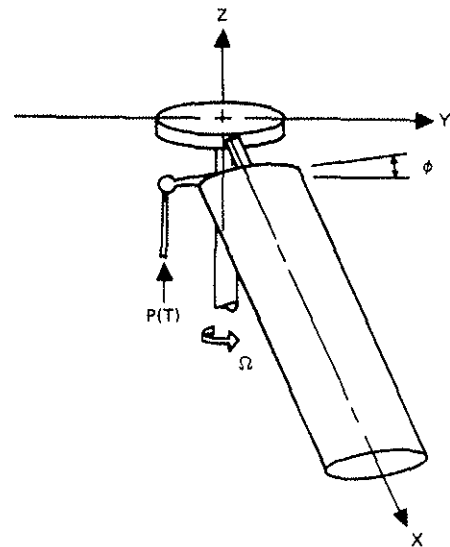


Figure I. 1. Rigid Blade, Rigid Pitch-Link Configuration

TABLE I. 1. MODEL ROTOR AND OH-6A BLADE DATA

Parameter	9-ft Model	OH-6A
I_{xx} N-m-sec ² /rad (in-lb _f -sec ² /rad)	0.0011 (0.01)	0.0508 (0.45)
Ω (rpm)	630	465
Ω (rad/sec)	65.97	48.69
R cm (inches)	3.6 (1.40)	15.4 (6.08)
P_o N (lb _f)	8.0 (1.8)	44.9 (10.1)